Structure and orientational behaviour of polyurethane containing polydimethylsiloxane

Mitsuhiro Shibayama*, Minoru Inoue, Tomoyuki Yamamoto and Shunji Nomura

Department of Polymer Science and Engineering, Kyoto Institute of Technology, Matsugasaki, Kyoto 606, Japan

(Received 10 April 1989; revised 6 May 1989; accepted 15 May 1989)

The structure and orientational behaviour of polyurethanes containing polydimethylsiloxane in the main chain was investigated by means of infrared dichroism, small angle light scattering and differential scanning calorimetry. It was found that the introduction of polydimethylsiloxane in the main chain reduced the crystallization capability of the soft segments. Hard and soft segments are oriented positively on uniaxial stretching. The orientational behaviour of the hard segments is different from that for most segmented polyurethanes and poly(urethaneurea)s, in which hard segments show negative orientation at low elongation. The difference in orientational behaviour is discussed in terms of the capability of self-cohesion of hard segments.

(Keywords: polyurethane; polydimethylsiloxane; infrared dichroism; orientation; spherulite

INTRODUCTION

The structure and orientational behaviour of multiblock copolymers, such as segmented polyurethanes and segmented poly(urethaneurea)s, has been investigated to account for the unique mechanical properties of these elastomers[1–12]. These polymers consist of hard and soft segments and usually form a microphase separated structure due to immiscibility of the two kinds of segment. Fourier transform infrared dichroism (*FT*i.r.d.) is one of the most powerful tools for studying segment orientation and the state of hydrogen bonding because one can work on a specific absorption band which is responsible for orientation and/or the state of hydrogen bonding.

It might be natural to expect both hard and soft segments in these elastomers to orient positively like rubber when they are stretched. Most of these elastomers, however, show different behaviour. Hard segments orient negatively at the beginning of stretching and then orient positively with increasing stretching. Several models have been proposed to account for this unique behaviour of hard segment orientation. Bonart *et al.*[6] presented a kind of floating rod model in a continuum medium. Hard segment lamellae with their long axis perpendicular to the segment direction orient in such a way that the long axis is along the stretching direction, resulting in negative orientation of the hard segments. Kimura *et al.*[2,7] and Shibayama *et al.*[11,12] showed a spherulite deformation model based on observation of spherulites. In this model, spherulites are deformed along the stretching direction and the contribution of positively oriented lamellae in the stretching direction becomes dominant. Since the hard segments are aligned perpendicular to the long axis of the lamellae, the hard segments become oriented negatively. When these polymers are highly deformed, both models predict that rods or spherulites are broken into small pieces, resulting in positive orientation for both hard and soft segments.

Segmented polyurethanes studies in this paper, designated as the KP series, however, do not show negative orientation of the hard segment on stretching though a spherulitic structure is observed with a polarized microscope and small angle light scattering. It is one of the objectives of this paper to investigate the orientational behaviour of KPs by combining *FT*i.r.d. with other techniques, such as differential scanning calorimetry (d.s.c.), mechanical measurements, small angle X-ray and light scattering.

KPs were synthesized by Kira *et al.*[13] as a medical material for artificial heart and blood vessels to improve antithrombogenicity without losing suitable mechanical properties and processability. KPs have a dimethylsiloxane component in the main chain. Kira *et al.* reported that antithrombogenicity and mechanical properties were optimized when the KPs contain 13 wt% poly(ethylene oxide)–poly(dimethylsiloxane)–poly(ethylene oxide) (PES).

In this paper, we investigate the structure and mechanical properties of KPs and discuss orientational behaviour from structural points of view.

EXPERIMENTAL

Samples

Segmented polyurethanes containing dimethylsiloxane in the main chain, called the KP-13 series, were supplied from Kanegafuchi Chemical Co. Ltd, Japan. As shown in *Table 1* and *Scheme 1*, KP-13 is composed of 55 wt% poly(tetramethylene glycol) (PTMG), 13 wt% poly(ethylene oxide)–polydimethylsiloxane–poly(ethylene oxide) (PES) and 32 wt% 4,4′-diphenylmethane diisocyanate (MDI) and ethylene glycol (EG). The molecular weight of PES was 2400, and the values of *a*, *b* and *c* in *Scheme*

* To whom correspondence should be addressed

0032-3861/90/040749-09

Table 1 Chemical composition of the KP series

Code	Soft segment molecular weights PTMG	PES	Weight fractions of PTMG:PES:(MDI+EG)
KP-0-3000	2900	0	68:0:32
KP-13-2000	2000	2400	55:13:32
KP-13-1000	1000	2400	55:13:32
KP-13-650	650	2400	55:13:32

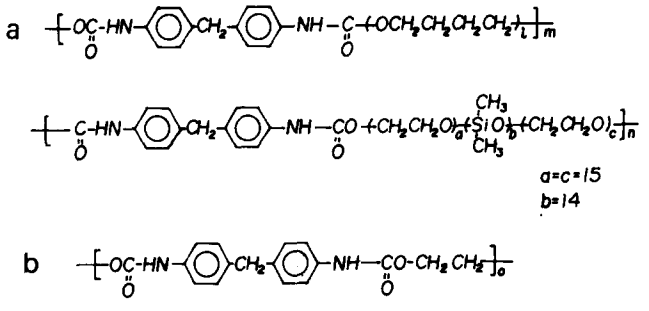

Scheme 1 Chemical structures of the KP series: (a) soft segment (MDI–PTMG, MDI–PES); (b) hard segment (MDI–EG)

l were determined to be, respectively, ≈15, ≈14 and ≈15 by ^{1}H nuclear magnetic resonance (n.m.r.) measurement of PES.

Since the details of sample preparation are reported by Kira *et al.*[13], the following is only a brief summary of sample preparation. A prepolymer was first prepared by polymerizing prescribed amounts of MDI, PTMG and PES in a solvent of a 7:3 mixture of dioxane and *N,N'*-dimethylacetamide at 50°C for 1 h. The chain was extended by adding EG at the same temperature and was reacted for 2 h.

The samples are coded as KP followed by the PES content in wt% and the molecular weight of PTMG. KP-0-3000 is a reference polyurethane which does not contain PES segments, as shown in *Table 1*. All of the samples were received in powder form.

KPs were dissolved in a mixed solvent of dioxane and *N,N'*-dimethyacetamide (7:3 in weight), cast onto a glass plate in the atmosphere of the solvent vapour at 60°C and then dried gradually. Films thus obtained were further dried in a vacuum oven for 3 days. Films ≈300 μm thick were used for all the experiments except infrared dichroism measurement. For infrared dichroism measurement, films ≈10 μm thick were used because of high infrared absorbance of the films. It was assumed that the film thickness dependence of the mechanical properties and structure was negligible.

Mechanical measurements

Stress–strain curve measurements were conducted with a Shimazu autograph IM-100 at 40 mm min^{-1} crosshead speed, 20°C and 65% relative humidity. The dimensions of the film between gauges were 30 mm long and 10 mm wide.

Dynamic viscoelastic properties were measured with a Rheospectoler Model DVE-V4, Rheology Co. Ltd, Kyoto. By loading a synthesized strain consisting of 2^n sine waves, where n is an integer between 0 and 8, temperature and frequency dispersion curves were obtained by a single temperature scan (5°C min^{-1}).

D.s.c. and TG

D.s.c. and thermal gravimetry (TG) thermograms were taken by using DSC Model 8230, Rigaku Denki Co. Ltd, and DT-30, Shimazu Co. Ltd, respectively. The temperature scanning rate was 10°C min^{-1} both for d.s.c. and TG. The samples were purged by nitrogen gas.

Small angle scattering

Small angle light scattering patterns were taken with a He–Ne laser having a wavelength of 632.8 nm. Small-angle X-ray scattering patterns were obtained with CuKα radiation operated at 40 kV and 27.5 mA. Exposure time was kept at 72 h.

Infrared dichroism

Infrared dichroism of the KP series was measured with a Firis 25 Fourier transform infrared spectrometer (Fuji Electric Co. Ltd) in an atmosphere of 40% relative humidity and at 20°C. The resolution was kept at 4 cm^{-1} throughout the experiments and spectra were accumulated 32 times.

RESULTS AND DISCUSSION

Mechanical properties

Figure 1 shows stress–strain curves of the KP series. KP-0-3000 has the highest strength and elongation at break. KP-13-2000 has comparable strength and elongation at break to KP-0-3000. The details of mechanical parameters are listed in *Table 2*. Kira *et al.*[13] reported that mechanical strength decreases with increasing PES content and that mechanical properties and antithrombogenicity are optimized at ≈13% PES content. With decreasing molecular weight of PTMG, all of the mechanical characteristic parameters, such as initial modulus, elongation and strength at break, decrease. *Figure 2* shows the work recovery efficiency, *W*, of the KP series, which is defined by

$$W = (S_{cont}/S_{draw}) \times 100 \quad (\%)$$

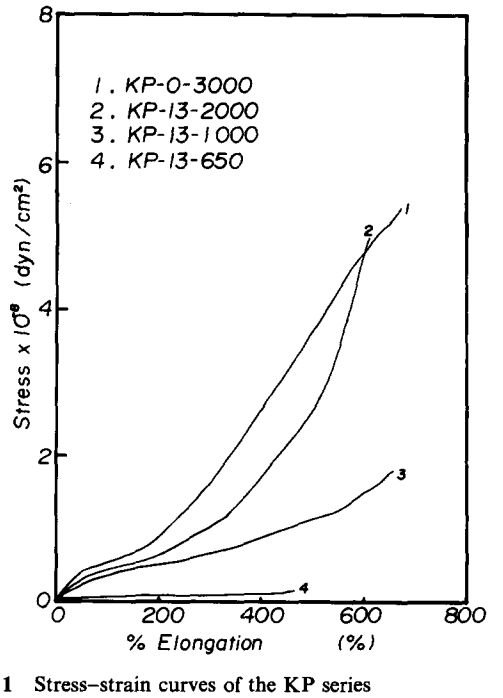

Figure 1 Stress–strain curves of the KP series

where S_{draw} and S_{cont} are the work done to the system and to the reservoir during drawing and contraction processes, respectively. This is easily obtained by evaluating the areas between the stress–strain curve and the abscissa up to a given elongation. As shown in *Figure 2*, for KPs except KP-13-650 work recovery efficiency depends strongly on percentage elongation. Relatively high work recovery efficiency at low elongation indicates that the system has a network structure like an elastomer in origin which is destroyed by large deformation. For KP-13-650, on the other hand, such a network structure hardly developed, resulting in plastic deformation.

Table 2 Tensile properties of the KP series

Code	$10^8 \times$ Strength at break (dyn cm^{-2})	Elongation at break (%)	$10^8 \times$ Modulus (dyn cm^{-2})
KP-0-3000	5.30	665	1.22
KP-13-2000	4.94	588	1.25
KP-13-1000	1.67	631	0.54
KP-13-650	0.19	458	0.21

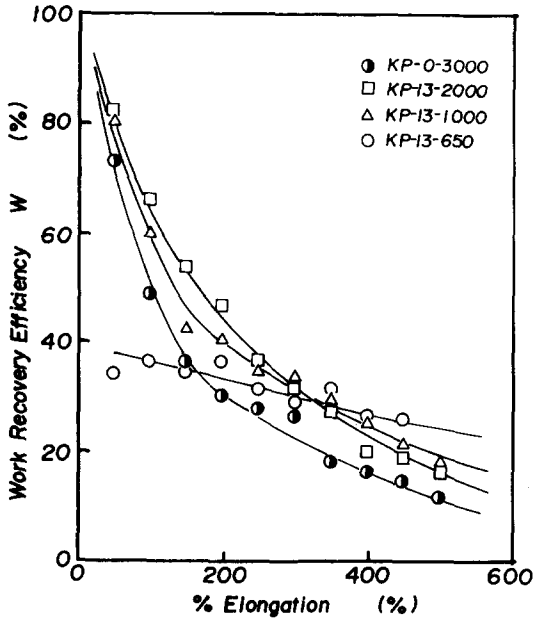

Figure 2 Percentage elongation dependence of work recovery efficiency, W

Figures 3a and *b*, respectively, show storage (E') and loss moduli (E'') of the KP series measured at 8 Hz as a function of temperature. The variation of the moduli clearly shows the presence of three regions: glassy (I), glass transition (II) and rubbery plateau (III).

In region I, the samples are in the glassy state. Although PTMG is a crystallizable polymer with a melting temperature of $\approx 0°C$, the soft segments are not in the crystalline state except for KP-0-3000, as will be discussed in the next section. In region II, peaks in E'' correspond to the glass transition of the soft segments. The glass transition temperature increases with decreasing soft segment molecular weight, indicating that the longer the soft segment, the better the phases are separated. In addition, broad peaks appear around $-40°C$ both in E' and in E'' for KP-0-3000. These are due to crystallization of the soft segment PTMG.

In region III, the rubbery plateau terminates at a temperature, T_t. This temperature may be related to the glass transition temperature of the hard segment, $T_{g,h}$, although $T_{g,h}$ is not observed by d.s.c., as will be discussed in the next section. T_t can be also considered to be the temperature at which the hard segment domains are disorganized and/or physical crosslinks consisting of the hard segments are broken[14]. It is interesting to note that the lower the soft segment molecular weight, the lower the T_t. This phenomenon can be explained as follows. With decreasing soft segment length, the miscibility of the soft and hard segments increases. Soft segments with a low molecular weight can penetrate the hard segment domains and/or some of the hard segments can be

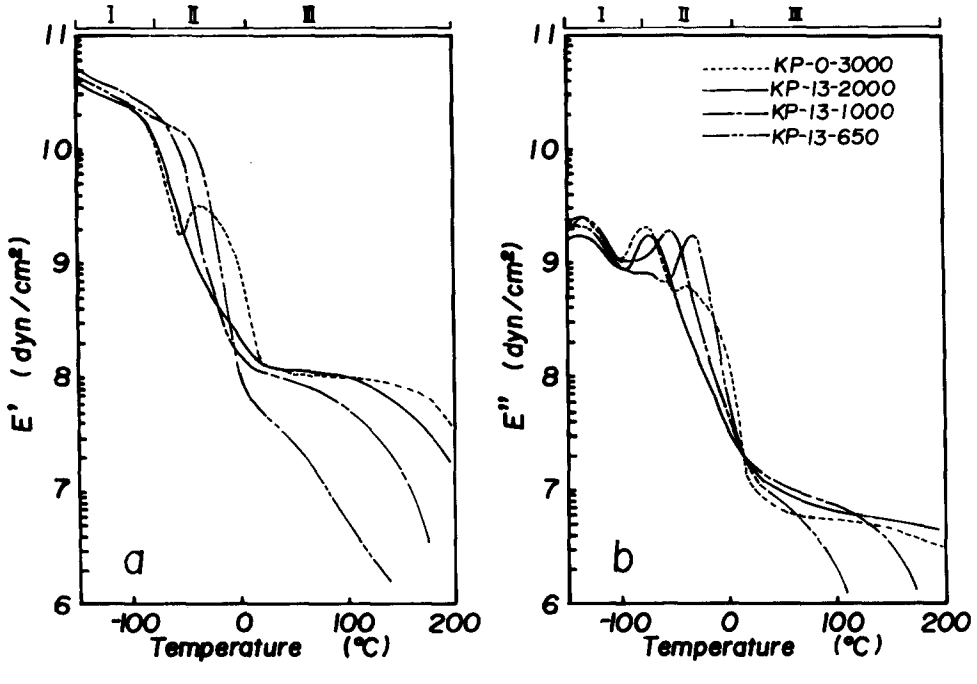

Figure 3 Temperature dependence of (a) dynamic mechanical storage modulus (E') and (b) loss modulus (E'') measured at 8 Hz

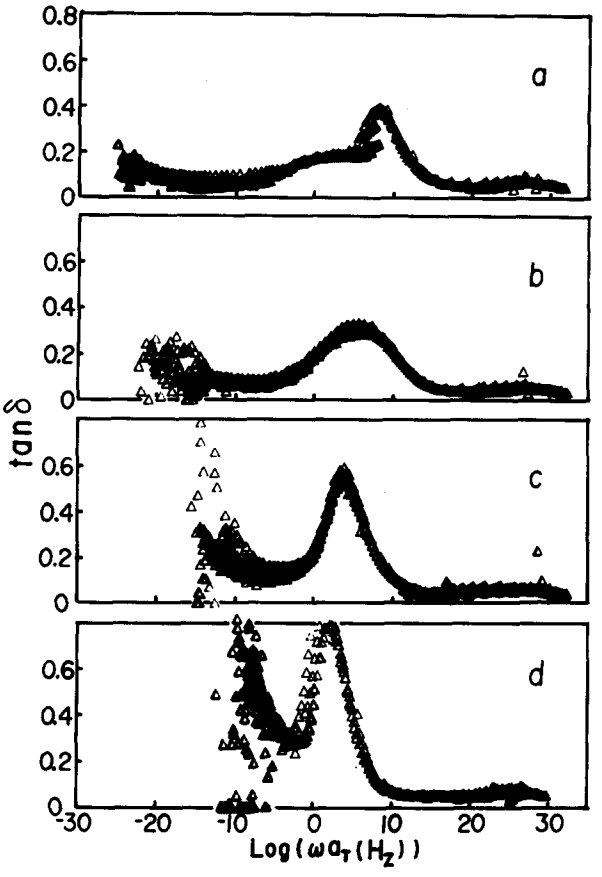

Figure 4 Frequency dispersion curves for (a) KP-0-3000, (b) KP-13-2000, (c) KP-13-1000 and (d) KP-13-650. The reference temperature was −5°C

dispersed in the soft segment matrix, resulting in a lowering of the cohesive power of the hard segment domains. Since the hard segment domains play a role as a physical crosslink, destruction of the hard segment induces fluidity of the system. Therefore, T_t depends upon the soft segment molecular weight.

It is also worthwhile to note that the storage modulus in region III is more or less the same for all KPs except KP-13-650. This shows that the volume fractions of the hard and soft segment phases do not vary so much in those samples and the connectivity of each phase is roughly equal since E' depends both on the volume fractions and on phase connectivity[15].

Figures 4a–d show frequency dispersions of tan δ for KP-0-3000, KP-13-2000, KP-13-1000 and KP-13-650, respectively. The reference temperature was taken to be −5°C. Each curve has a dispersion maximum due to the glass transition temperature, the position of which moves from the high frequency side to the low frequency side with decreasing soft segment molecular weight. This is consistent with the result of *Figure 3*. For KP-0-3000, a broad shoulder is present near the dispersion peak of the glass transition. This corresponds to the melting of the soft segments.

Note that KP-13-2000 has a broader dispersion peak than the others. Since KP-13-2000 is expected to be better phase separated than KP-13-1000 and KP-13-650, as discussed above, this broadness is partially due to soft segment melting.

Figure 5 shows the reciprocal temperature dependence of the horizontal shift factor a_T, which was used to construct *Figure 4*. As can be seen, there are at least two dispersion mechanisms. These are assigned as the glass transition of the soft segments (β dispersion) and local chain motion which appears around −120°C (γ dispersion)[14]. The apparent activation energies for the β and γ dispersions are, respectively, around 40 kcal mol^{-1} and 20 kcal mol^{-1}, as listed in *Table 3*. These values are in good agreement with literature values[11,14].

Thermal properties

Figure 6 shows d.s.c. (solid line) and TG (dashed line) thermograms of the KP series. $T_{g,s}$, $T_{m,s}$ and $T_{m,h}$ denote the glass transition and melting temperatures of the soft segment and the melting temperature of the hard segment, respectively. These characteristic temperatures are listed in *Table 4*. The hard segment glass transition temperature, $T_{g,h}$, was not observed in the thermograms. The absence of $T_{g,h}$ might be due to the fact that disorganization of the hard segment domains occurring at a wide temperature range between 0 and 200°C conceals the change in heat capacity due to the glass transition of the hard segment. Note that only KP-0-3000 shows a distinct endotherm due to melting of the soft segment. This indicates that soft segment domains are well developed for KP-0-3000 compared with the other KP series with a siloxane component. The glass transition temperature of the soft segments, $T_{g,s}$, decreases with increasing soft segment molecular weight, indicating that the hard and soft segment domains tend to mix more with lowering soft segment molecular weight. All of these temperatures are very close to those observed by viscoelastic measurements as shown in *Figure 3*. The presence of polydimethylsiloxane in the main chain seems to accelerate domain mixing. TG thermograms indicate that thermal degradation starts around the hard segment melting temperature, $T_{m,h}$.

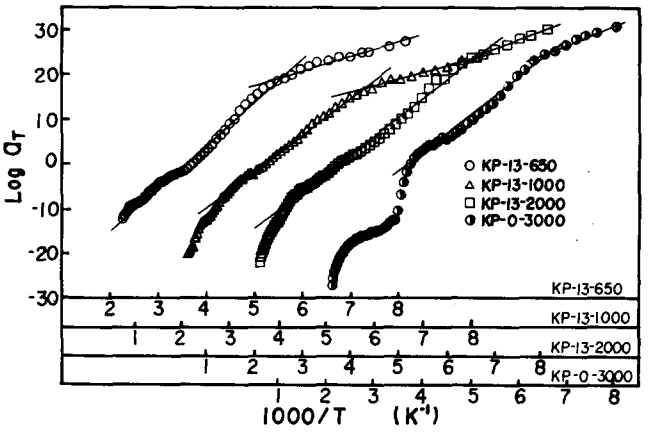

Figure 5 Arrhenius plots of the apparent activation energies of the shift factor, a_T

Table 3 Apparent activation energies of mechanical dispersion

Code	Activation energy (kcal mol^{-1})	
	β	γ
KP-0-3000	38.4	19.7
KP-13-2000	38.2	19.4
KP-13-1000	37.3	13.4
KP-13-650	44.2	15.2

SAXS and SALS

Figure 7 shows the SAXS patterns for non-stretched and 150% stretched KPs. No specific features, such as diffraction maxima related to the long spacing of lamellae, were resolved in the patterns for non-stretched KPs. In the pattern for the 150% stretched film, two- or four-point patterns are seen in the stretching direction, indicating concentration of the hard segment lamellae along that direction. We reported previously that the lamellar spacing was clearly seen in SAXS patterns for segmented poly(urethaneurea)s (SPUU) and these became a four-point pattern by stretching[12]. D.s.c. and viscoelastic measurements on both the KP series, except for KP-13-650, and SPUU revealed that the two systems had a well developed phase separated structure. No indication of two-phase structure was observed by SAXS.

Small angle light scattering (SALS) H_v patterns for non-stretched and stretched KPs are shown in *Figure 8*. *P*, *A* and *ED* respectively show the directions of polarizer, analyser and elongation. For non-stretched films, only KP-0-3000 shows a clear four-leaf pattern indicating the presence of spherulitic texture of radius 3.4 μm in the system. KP-0-3000 shows a typical change in SALS patterns on stretching, i.e. spherulite deformation due to uniaxial stretching. The spherulites are deformed along *ED*, giving rise to a flattened pattern along the equatorial direction. In contrast, KP-13-2000 and KP-13-1000 show no characteristic patterns when they are undeformed. With increasing percentage elongation they begin to show a cross pattern in which the scattered intensity monotonically decreases with scattering angle. This indicates the development of sheaf or rodlike superstructure of which the dimension is of the order of

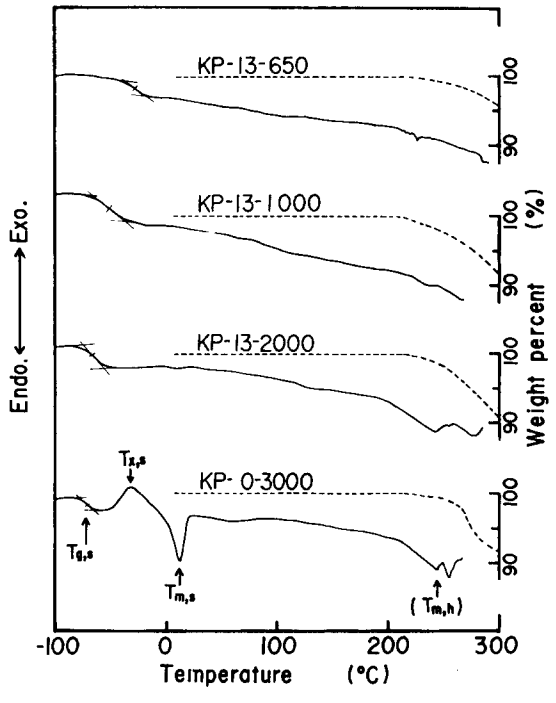

Figure 6 D.s.c. and TG thermograms of the KP series

Table 4 Characteristic temperatures[a] of KP series obtained by d.s.c.

Code	$T_{g,s}$ (°C)	$T_{x,s}$ (°C)	$T_{m,s}$ (°C)	$T_{m,h}$ (°C)
KP-0-3000	−71.7	−32.4	10.5	234
KP-13-2000	−70.7	—	—	232
KP-13-1000	−50.1	—	—	219
KP-13-650	−31.5	—	—	—

[a] $T_{g,s}$, glass transition temperature of the soft segments; $T_{x,s}$, crystallization temperature of the soft segments; $T_{m,s}$, melting temperature of the soft segments; $T_{m,h}$, melting temperature of the hard segments

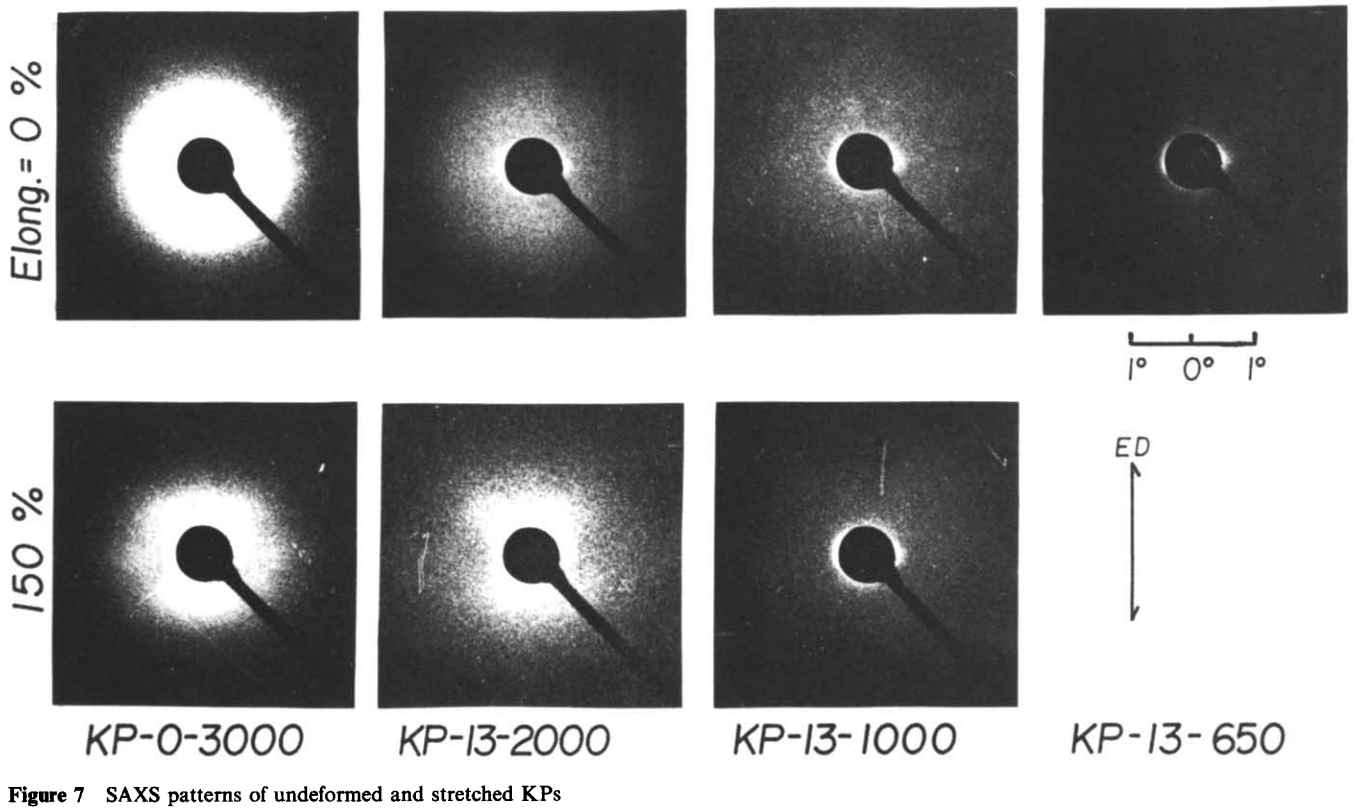

Figure 7 SAXS patterns of undeformed and stretched KPs

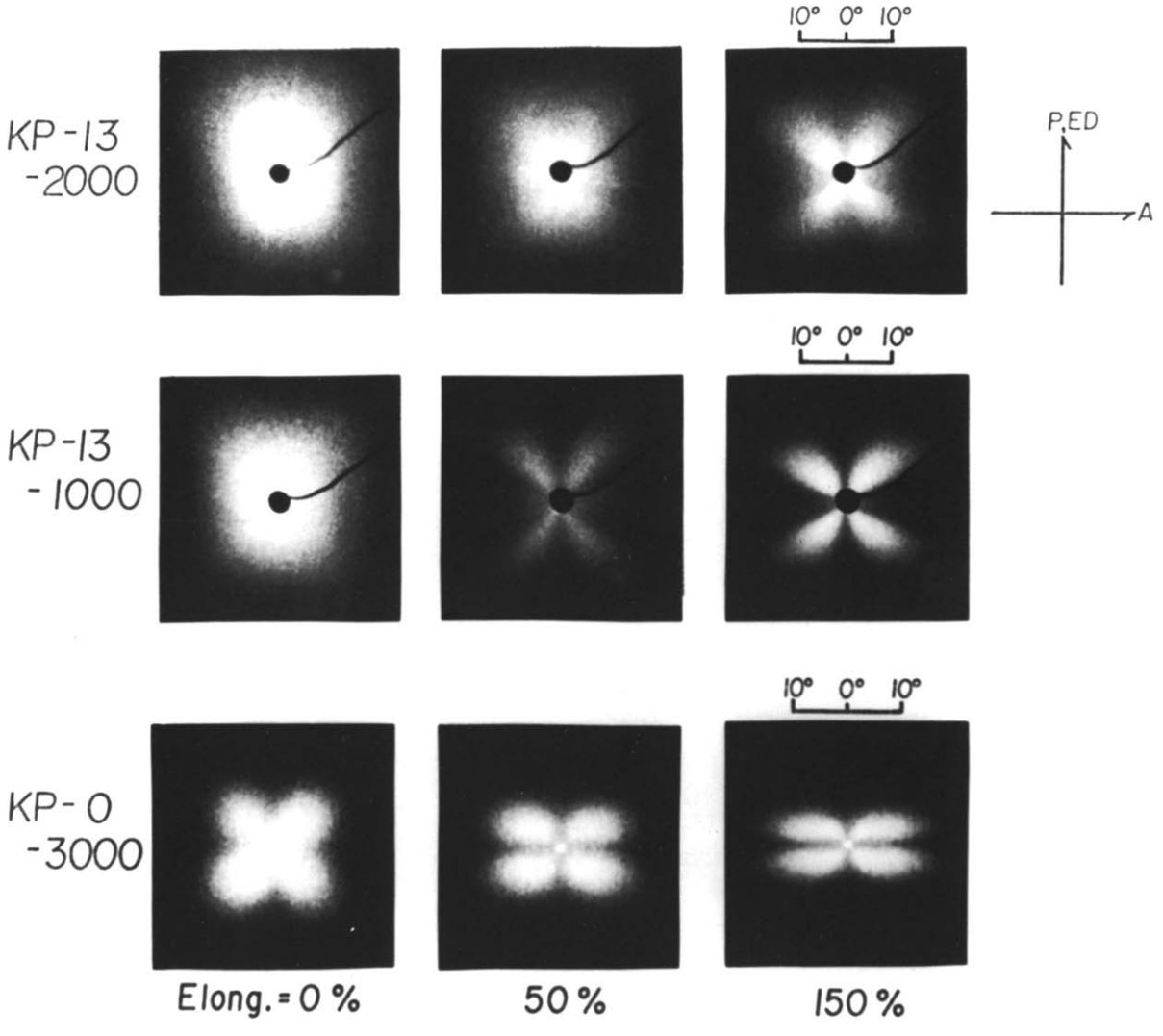

Figure 8 SALS patterns of undeformed and stretched KPs

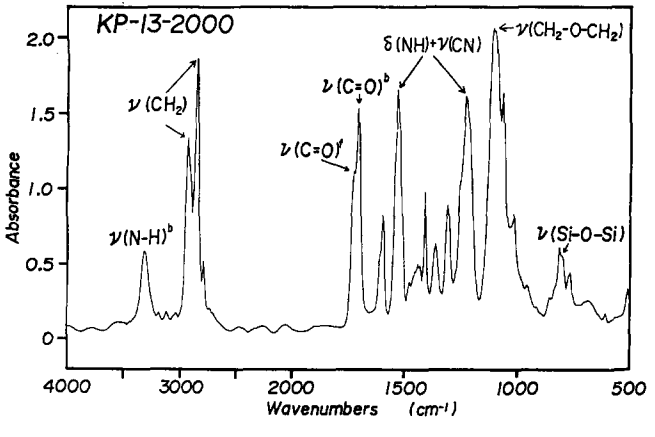

Figure 9 Survey of absorption spectrum of KP-13-2000

micrometres. The appearance of the cross pattern is due to strain-induced crystallization of the soft segments since crystalline diffraction from (110) and (020) planes of PTMG crystals were observed for stretched KP-13-2000. Similar patterns were observed for tubular extruded polybutene-1 films[16].

Table 5 Assignment and abbreviation of absorption bands

Wavenumber (cm^{-1})	Abbreviation	Assignment
804	ν(Si–O–Si)	SiO stretching
1109	$\nu(CH_2–O–CH_2)$	Ether stretching
1228	δ(NH)+ν(CN)	Bending of urethane NH and CN
1536	δ(NH)+ν(CN)	Bending of urethane NH and CN
1709	$\nu(C{=}O)^b$	Hydrogen bonded carbonyl stretching
1730	$\nu(C{=}O)^f$	Free carbonyl stretching
2858	$\nu(CH_2)$	Methylene stretching
2941	$\nu(CH_2)$	Methylene stretching
3322	$\nu(NH)^b$	Hydrogen bonded NH stretching

Fourier transform infrared dichroism (FT*i.r.d.*)

Figure 9 shows a survey spectrum of KP-13-2000. All of the KPs except KP-0-3000 show similar spectra. The absorption band due to silica is missing only in the spectrum of KP-0-3000. Most of the characteristic absorption bands are assigned as listed in *Table 5*. We focus on the NH stretching band, ν(NH), the stretching band of the methylene group, $\nu(CH_2)$ and free and bonded urethane carbonyl bands, $\nu(C{=}O)^f$ and

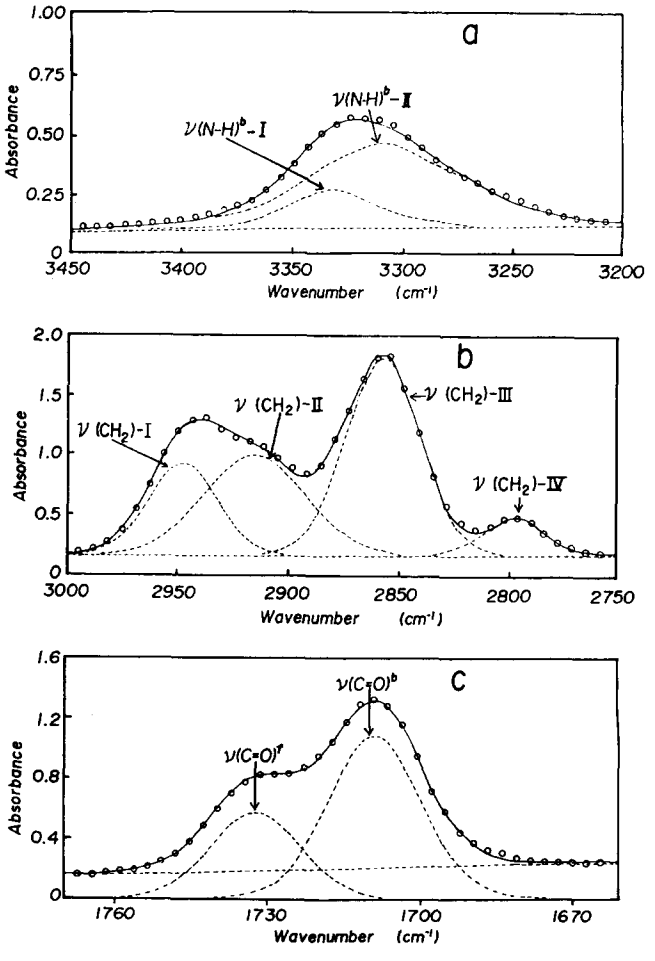

Figure 10 *FT*i.r. spectra of (a) NH stretching band, (b) stretching band of methylene group and (c) carbonyl band. o, Observed and, ——, calculated spectra; – – –, individual components of absorption bands

$\nu(C{=}O)^b$, respectively, for evaluation of the soft and hard segment orientations and degree of hydrogen bonding.

Figure 10 shows examples of peak resolving of *FT*i.r. absorption spectra. The spectra were resolved into several symmetric peaks composed of Gaussian and Lorentzian components. The details of the curve resolving will be discussed in a forthcoming paper[17]. In the NH stretching region (*Figure 10a*), the hydrogen bonded NH stretching band was decomposed to $\nu(NH)^b$-I and $\nu(NH)^b$-II. The difference in wavenumbers between I and II may be due to the difference in the state of hydrogen bonding as discussed by Skrovanek *et al.*[18] in the case of hydrogen bonding with amide groups. In the absorption region of stretching of the methylene group (*Figure 10b*), $\nu(CH_2)$ is resolved into four peaks designated by I–IV. Although peaks I and III are well defined as the stretching bands of the methylene group, peaks II and IV are introduced to minimize the error of curve resolving. Therefore, these bands have not yet been completely assigned. In the carbonyl region (*Figure 10c*), the bonded and free carbonyl bands, $\nu(C{=}O)^b$ and $\nu(C{=}O)^f$, are successfully resolved.

Figure 11 shows the percentage elongation dependence of the index of hydrogen bonding, H_{UT}, which is defined as follows:

$$H_{UT} = \frac{A[\nu(C{=}O)^b]}{A[\nu(C{=}O)^b] + A[\nu(C{=}O)^f]}$$

Note that H_{UT} is not a quantitative measure of the fraction of hydrogen bonding since the absorption coefficient of neither $\nu(C{=}O)^b$ nor $\nu(C{=}O)^f$ has been precisely evaluated. As shown in the figure, H_{UT} is highest for KP-0-3000 and decreases with decreasing soft segment molecular weight. This indicates that KP-0-3000 is well phase separated and the cohesive power of the hard segment domains is highest among the three. H_{UT} for KP-13-650 could not be evaluated due to scattering of data points. The order of the values of H_{UT} is well correlated with the results of the mechanical and thermal properties discussed above. It is of interest that H_{UT} remains constant with increasing percentage elongation. If phase mixing is developed due to stretching, one expects a decrease in H_{UT} because of decreasing hydrogen bonding in the hard segment domains. The result indicates that a decrease in hydrogen bonding between hard segments is compensated by an increase in hydrogen bonding between hard and soft segments. This phenomenon is observed in segmented poly(urethaneurea)s where hydrogen bonding indices for urethane and urea carbonyl groups are independently evaluated by focusing on the corresponding absorption bands; this will be reported in a forthcoming paper[17].

Figure 12 shows percentage elongation dependence of the orientation factors of NH and CH_2 groups. These were estimated from *FT*i.r.d. Although absorption peak heights were used to evaluate dichroism in previous papers[11,12], the areas of the corresponding absorption bands were used here to improve accuracy. Since NH and CH_2 groups are mainly on the hard and soft segments, respectively, the orientations of these groups indicate the orientations of the hard and soft segments. A negative sign of the orientation factor means positive orientation of the hard and soft segments because dipole moments of both NH and CH_2 groups are oriented roughly perpendicular to the direction of the segments. With increasing percentage elongation, both orient negatively. Hence both hard and soft segments are oriented positively with increase in percentage elongation. KP-13-650, however, shows almost no orientation. This is due to the fact that the hard segment domains are not well developed to behave as physical crosslink points. In addition, the soft segments are not long enough to entangle each other. Although the molecular weight of the soft segment block chains between hard segments is not evaluated quantitatively, it must be significantly

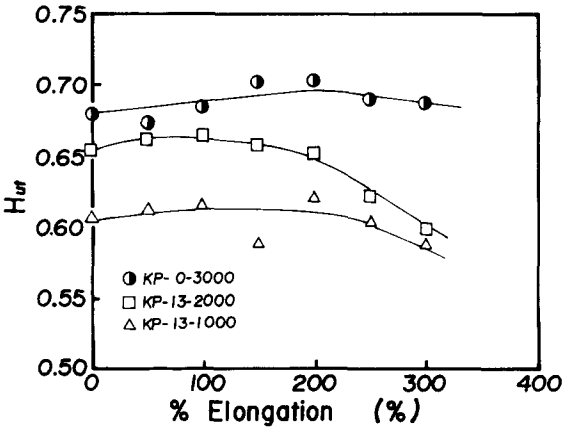

Figure 11 Percentage elongation dependence of hydrogen bond index, H_{UT}

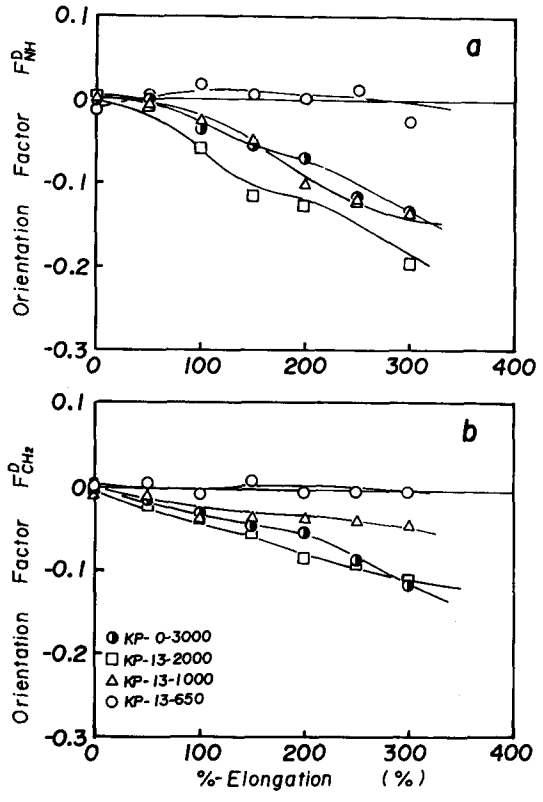

Figure 12 Percentage elongation of orientation factors of (a) NH group, F^D_{NH} and (b) CH_2 group, F_{CH_2}, observed at 20°C

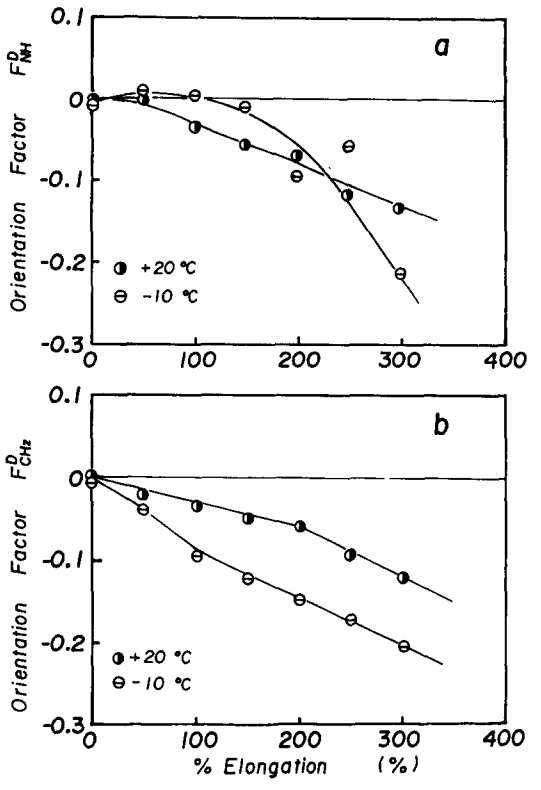

Figure 13 Percentage elongation dependence of orientation factors of (a) NH group, F^D_{NH} and (b) CH_2 group, F_{CH_2}, of KP-0-3000 observed at 20°C and −10°C

smaller for KP-13-650 than for KP-13-1000, KP-13-2000 and KP-0-3000. The positive orientation behaviour of the hard segments is completely different from the behaviour observed in segmented poly(urethane-urea)s[2,7,11,12] and polyurethanes[6], of which hard segments show negative orientation at the beginning of stretching. The negative orientation of the hard segments is explained with superstructures like rods and/or spherulites. We reported previously that hard segments in segmented poly(urethaneurea)s and segmented polyurethanes show negative orientation when they have superstructures like rods and/or spherulites[11,12]. KP-0-3000 shows, however, positive orientation of the hard segments from the beginning of stretching although it has spherulitic superstructure. To solve this contradiction, we measured percentage elongation dependence of the orientation factors of the hard and soft segments by varying temperature.

Figure 13 shows percentage elongation dependence of orientation factors of NH and CH_2 groups for KP-0-3000 measured at 20 and −10°C. As shown in the figure, a trend of negative orientation of the hard segment (positive orientation of NH groups) is seen at −10°C. On the other hand, soft segments are more oriented at −10 than at 20°C. This indicates that with lowering temperature the cohesive power which binds the hard segment domains increases, giving rise to more elastic deformation, and superstructures become less destroyed on stretching. For KP-13-2000, no trend of negative orientation of the hard segment was observed even at −10°C. Absence of negative orientation behaviour of the hard segment for KPs containing siloxane components results from low cohesive power of the hard segments.

CONCLUSION

The mechanical and orientational behaviour of segmented polyurethane with a polydimethylsiloxane component in the main chain was investigated. By comparison with a reference sample, KP-0-3000, which does not contain a siloxane component, the presence of the siloxane component reduces the crystallization capability of the soft segments. Glass transition measurements reveal that the longer the soft segment molecular weight, the better are phases separated, as often observed in segmented polyurethanes and segmented poly(urethaneurea)s. The KPs show no negative orientation of hard segments when stretched. Both hard and soft segments are oriented positively from the beginning of stretching, which is completely different from the behaviour reported in the literature for SPU and SPUU. Hard segments, however, start to orient negatively on stretching when measured at low temperature. KPs are, therefore, classified as polyurethanes with low cohesive power of the hard segments.

ACKNOWLEDGEMENTS

The authors are grateful to Dr K. Kira and Dr K. Hiramatsu, Central Research, Kanegafuchi Chemical Co. Ltd, for supplying the segmented polyurethanes studied in this work. Thanks are due to Resources and Environment Protection Research Laboratory, NEC Corporation, Kawasaki, Japan for financial assistance.

REFERENCES

1 Cooper, S. L. and Seymour, R. W. in 'Block and Graft Copolymers' (Eds J. J. Burke and V. Weiss), Syracuse University Press, New York, 1973

2 Kimura, I., Ishihara, H., Ono, H., Yoshihara, N., Nomura, S. and Kawai, H. *Macromolecules* 1974, **7**, 355
3 Sung, C. S. P., Smith, T. W. and Sung, N. H. *Macromolecules* 1980, **13**, 117
4 Laptij, S. V., Lipatov, Yu. S., Kercha, Yu. Yu., Kosenko, L. A., Vatulev, V. N. and Gaiduk, R. L. *Polymer* 1982, **23**, 1917
5 Brunette, C. M., Hsu, S. L. and MacKnight, W. J. *Macromolecules* 1982, **15**, 71
6 Hoffman, K. and Bonart, R. *Makromol. Chem.* 1983, **184**, 1529
7 Ishihara, H., Kimura, I. and Yoshihara, N. *J. Macromol. Sci. Phys.* 1983–1984, **B22**, 713
8 Wang, C. B. and Cooper, S. L. *Macromolecules* 1983, **16**, 775
9 Miller, J. A., Lin, S. B., Hwang, K. K. S., Wu, K. S., Gibson, P. E. and Cooper, S. L. *Macromolecules* 1985, **18**, 32
10 Desper, C. R., Schneider, N. S., Jasinski, J. P. and Lin, J. S. *Macromolecules* 1985, **18**, 2755
11 Shibayama, M., Kawauchi, T., Kotani, T., Nomura, S. and Matsuda, T. *Polym. J.* 1986, **18**, 719
12 Shibayama, M., Ohki, Y., Korani, T. and Nomura, S. *Polym. J.* 1987, **19**, 1067
13 Kira, K., Minokami, T., Yamamoto, N., Hayashi, K. and Yamashita, I. *Seitaizairyo* (*Biomaterials*) 1983, **1**, 29
14 Ferguson, J., Hourston, D. J., Meredith, R. and Patsavoudis, D. *Eur. Polym. J.* 1972, **8**, 369
15 Nielsen, L. E. 'Mechanical Properties of Polymers and Composites', Marcel Dekker, New York, 1975
16 Hashimoto, T., Todo, A., Tsukahara, Y. and Kawai, H. *Polymer* 1979, **20**, 636
17 Yamamoto, T., Shibayama, M. S. and Nomura, S. *Polym. J.* 1989, **21**, 895
18 Skrovanek, D. J., Howe, S. E., Painter, P. C. and Coleman, M. M. *Macromolecules* 1985, **18**, 1676